Deuterium dissociation on ordered Sn/Pt(111) surface alloys

Cite as: J. Chem. Phys. **109**, 3255 (1998); https://doi.org/10.1063/1.476916
Submitted: 03 November 1997 . Accepted: 15 May 1998 . Published Online: 30 September 1998

P. Samson, A. Nesbitt, B. E. Koel, and A. Hodgson

Deuterium dissociation on ordered Sn/Pt(111) surface alloys

P. Samson and A. Nesbitt
Surface Science Research Centre, Liverpool University, Liverpool L69 3BX, United Kingdom

B. E. Koel
Department of Chemistry, University of Southern California, Los Angeles, California 90089-0482

A. Hodgson[a)]
Surface Science Research Centre, Liverpool University, Liverpool L69 3BX, United Kingdom

(Received 3 November 1997; accepted 15 May 1998)

We have explored the effect of alloying an unreactive metal, Sn, on the dynamics of D_2 dissociative chemisorption at Pt(111). By comparing D_2 sticking and recombinative desorption on Pt(111) with that on the ordered $p(2\times2)$ Sn/Pt(111) and $(\sqrt{3}\times\sqrt{3})R30°$ Sn/Pt(111) surface alloys, we examine the influence of the local surface composition on reactivity. The energy dependence of D_2 sticking $S(E)$ has been measured for all three surfaces using a hyperthermal beam. We find that the activation barrier for dissociative chemisorption is low on the $p(2\times2)$ alloy, but the sticking probability is reduced, compared to Pt(111), by an increase in the steric constraint on the dissociation site. Sticking on the $(\sqrt{3}\times\sqrt{3})R30°$ alloy is inefficient at thermal energies with a threshold of ~280 meV, below which the sticking probability falls exponentially. The increase in the barrier to D_2 dissociation occurs as the stable, high coordination Pt_3–D binding sites are lost by formation of the $(\sqrt{3}\times\sqrt{3})R30°$ alloy. Despite the large activation barrier, sticking is dominated by the vibrational ground state with the barrier occurring in the entrance channel, before the D_2 bond has stretched. Departures from a normal energy scaling indicate that the dissociation site is localized in the unit cell and we suggest favorable dissociation sites on the alloy surfaces. Estimates for the heats of adsorption, obtained by comparing activation energies to adsorption and desorption, indicate an abrupt decrease in the D binding energy as the Pt_3 sites are lost. We show that sticking and desorption parameters are consistent with an increasing steric constraint for adsorption/desorption on the alloy surfaces as the Sn content is increased and an increase in the barrier to dissociation as the stable Pt_3 sites are lost by alloying. © *1998 American Institute of Physics.* [S0021-9606(98)02031-5]

I. INTRODUCTION

Alloying metals provides a simple way to modify the reactivity of surfaces, allowing the kinetic and thermodynamic properties of an adsorbate to be modified to optimize the chemistry of a catalytic system.[1] While such materials are often complex, multicomponent systems, ordered bimetallic surface alloys offer an opportunity for detailed experiments to determine the influence of alloying on the dynamics of simple surface reactions. Sn forms a series of ordered surface alloys on Pt(111), whose structure depends on the initial Sn coverage. The first alloy, with a fractional Sn coverage of $\Theta_{Sn}=0.25$ monolayer (ML), has a $p(2\times2)$ low energy electron diffraction (LEED) pattern and a structure corresponding to the (111) plane of Pt_3Sn. The second surface alloy (hereafter the $\sqrt{3}$ alloy) has a composition Pt_2Sn, with a Sn coverage of $\Theta_{Sn}=0.33$ ML and a $(\sqrt{3}\times\sqrt{3})R30°$ LEED pattern. At intermediate Sn coverages a mixed $p(2\times2)$ and $(\sqrt{3}\times\sqrt{3})R30°$ LEED pattern is observed corresponding to domains of each alloy. These structures (Fig. 1) are true surface alloys, comprised of a single layer of alloy with the Sn adatoms buckled out of the surface by ~0.22 Å,[2,3] the structures having recently been confirmed by LEED $I-V$ calculations[4] and x-ray forward scattering measurements.[5] Such two-dimensional surface arrays, composed of an inert metal, Sn, alloyed into a reactive Pt(111) surface, may be expected to display a strong surface site dependence for dissociative chemisorption as well as electronic modification of the Pt reactivity.

LDA calculations by Hammer *et al.*[6,7] have shown that the barrier to H_2 dissociation across the transition metal series can be correlated to filling of the antibonding $(H_2 1\sigma_g - d)^*$ orbital, the barrier increasing as the d band falls in energy and the antibonding level fills. Dissociation of H_2/D_2 on transition metals[8] such as Ni,[9] Pt,[10] and Fe[11,12] is facile but becomes increasingly activated for metals such as Cu[13] and Ag[14] where the d band lies well below the Fermi level. For Pt(111) and Fe(110) sticking occurs at thermal energies and a steady increase in sticking probability with translational energy is observed, reflecting dissociation over a distribution of barriers corresponding to different collision geometries, molecular orientations, and sites in the surface unit cell. Noble metals on the other hand have filled d-bands and are characterized by large activation barriers to H_2/D_2 dissociation,[8] while sticking shows a threshold behavior, becoming efficient over a relatively narrow range of

a)FAX: 0151 708 0662; electronic mail: andrewh@ssci.liv.ac.uk

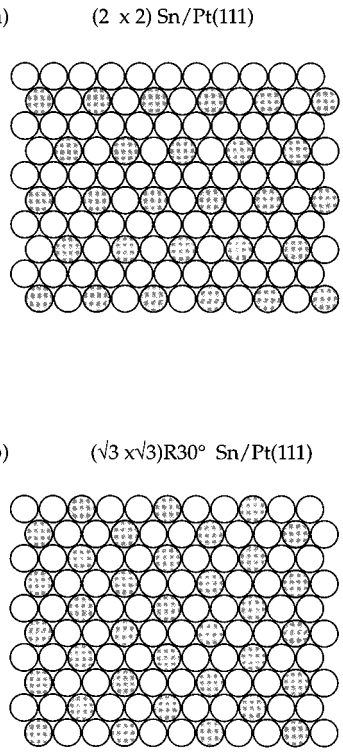

FIG. 1. Structure of the Sn/Pt(111) surface alloys.[3] The Sn (dark circles) is confined to the surface layer and induces a slight buckling of the top layer to accommodate the larger Sn atoms.

energy.[13,14] Similarly, Al surfaces have no *d* electron density of states at the Fermi level and have an extremely high barrier to H_2 dissociation.[15] Substitution of a metal with no *d*-band holes into a transition metal surface may alter the reactivity of the surface towards H_2 dissociation by modifying the local surface electronic structure as well as by blocking adsorption sites. The NiAl alloy, for example, has a full *d* band lying 1.8 eV below the Fermi level and H_2 dissociation on the NiAl(110) surface remains activated.[7,16] LDA potentials for dissociation of H_2 on the Cu(111), Cu_3Pt(111), and Pt(111) surfaces show that the local electronic structure on both the Cu and the Pt is perturbed by alloying, with the barrier increasing on the Cu sites and adsorption becoming less favorable on the Pt sites compared to Pt(111).[6]

Verbeek and Sachtler[17] investigated chemisorption on Pt_3Sn, PtSn, and $PtSn_2$ powders and found that adsorption of D_2 was strongly inhibited by alloying Pt with Sn. Koel and co-workers have shown that formation of the Sn/Pt surface alloys strongly modifies the selectivity and activity of Pt(111) for dehydrogenation,[18] the different surface alloys showing quite specific chemistry, presumably related to the changing stability of both the hydrocarbon and hydrogen species on the surface. Here we investigate how alloying Sn into the Pt(111) surface changes the reactivity of the surface to D_2. The formation of two different ordered surface alloys allows us to examine the effect of the local surface structure on the activation barrier and steric requirements for dissociation. We have measured sticking probabilities $S(E)$ on the Pt(111), $p(2\times2)$, and $\sqrt{3}$ alloy surfaces and report activation energies and preexponential factors for D_2 recombinative desorption, obtained from thermal desorption measurements. The adsorption and desorption processes are related by detailed balance and the results are consistent with an adsorption/desorption site which becomes increasingly constrained as the Sn content of the surface increases. The binding energy of D on the surface decreases for the $\sqrt{3}$ alloy as the stable Pt_3 binding sites are lost and dissociation becomes activated with a sterically constrained transition state.

II. EXPERIMENT

Experiments were carried out in an UHV chamber with a base pressure of $<5\times10^{-11}$ Torr, equipped with a three stage, differentially pumped molecular-beam source, surface cleaning, and characterization facilities.[11] The Sn deposition source was a resistively heated crucible made from Ta foil, operated at ~1100 K. The Pt(111) sample was cleaned *in situ* by repeated cycles of argon ion bombardment (500 eV, $\sim6\ \mu A\ cm^{-2}$) at 1000 K, heating to 670 K in oxygen ($<5\times10^{-7}$ Torr), and annealing at 1273 K until it showed a sharp LEED pattern and reproduced D_2 TPD spectra consistent with those in the literature. The Sn/Pt(111) surface alloys were prepared by vapor deposition of Sn onto the clean Pt(111) surface and annealing the sample to 1000 K. Depending upon the initial Sn coverage, the annealed surface exhibited a $p(2\times2)$, a $(\sqrt{3}\times\sqrt{3})R30°$, or a mixed LEED pattern, as described previously.[2] The D_2 molecular beam was produced by supersonic expansion using a Mo nozzle source operating at temperatures up to 2100 K and a backing pressure of 5 bar D_2. Translational energy distributions of D_2 were measured by time-of-flight using resonance-enhanced multiphoton ionization, mean translational energies for pure D_2 beams being related to the nozzle temperature T_n by the expression $E=(5.5/2)kT_n$ for the expansion conditions used here.[14] Translational energies above 500 meV were attained by seeding the D_2 molecular beam with H_2.

D_2 sticking on the clean Pt(111) surface, the $p(2\times2)$ and the $\sqrt{3}$ surface alloys were measured at a surface temperature of 150 K. Temperature programmed desorption (TPD) measurements were made by monitoring the recombinative desorption of D_2 from the front surface of the sample into a shrouded quadrupole mass spectrometer (QMS) whose entrance aperture was placed 3 mm from the spot where the molecular beam hit the sample. This was necessary to discriminate effectively against gas adsorbed on the sides and rear of the reactive Pt(111) crystal when measuring sticking on the unreactive alloy surfaces. During measurements of relative sticking probabilities, a D atom coverage of <3% was accumulated on the surface, while the relative D_2 exposure was determined using a second QMS in the main chamber to measure the flux in the molecular beam. The coverage of D atoms was then determined from the area of the thermal desorption peak for D_2. Absolute sticking probabilities were obtained from TPD/exposure measurements by using the direct reflection technique at high energy to calibrate measurements on the alloy surfaces.

III. RESULTS AND DISCUSSION

The results will be discussed under four headings. In Sec. III A, we describe the results of thermal desorption measurements from which we obtain activation energies and preexponential factors for recombinative desorption (Sec. III B). Measurements of the translational energy dependence of D_2 dissociative chemisorption are reported in Sec. III C, and we discuss the energy scaling for the $\sqrt{3}$ alloy surface and a simple model for the energy dependence $S(E)$. In Sec. III D we calculate effective activation energies for sticking which allow us to estimate the overall energetics of D_2 adsorption on the three different surfaces.

A. Desorption measurements

Thermal desorption spectra from the bare Pt(111) sample and the two Sn/Pt(111) alloys were measured following exposure of the surfaces to a beam of pure D_2 at a surface temperature $T_s = 150$ K. A range of D atom coverages was achieved by varying both the exposure and the incident beam energy. TPD spectra as a function of D atom coverage are shown in Figs. 2(a)–2(c) for desorption from Pt(111), $p(2\times2)$, and $\sqrt{3}$ alloy surfaces, respectively, and are similar to those reported previously.[19–22] The D atom coverages on the Pt(111) surface have been determined from the relative areas of the D_2 desorption peaks, assuming a saturation coverage of $\Theta_D = 0.8$ ML.[19,22] The coverages on the alloy surfaces were normalized to the same desorption integral and showed a saturation coverage of 0.68 and 0.67 ML for the $p(2\times2)$ and $\sqrt{3}$ surfaces, respectively, taken at a nozzle temperature of 1275 K. This is larger than the 0.5 ML reported for these surfaces using atom dosing,[21] probably reflecting the influence of the Eley–Rideal reaction channel.

The peak desorption temperature decreases with increasing D atom coverage for all three surfaces and desorption is approximately second order. Desorption from Pt(111) occurs with a peak temperature of 350 K at low coverage, decreasing to 285 K and then broadening, with the peak shifting to 260 K as the coverage is increased towards saturation. For desorption from the $p(2\times2)$ alloy the desorption peak temperature is slightly higher, 375 K at low coverage, and decreases to 340 K as the coverage is increased. The desorption peak from the saturated surface has a broad low-temperature tail extending to 175 K. The peak desorption temperature for the $\sqrt{3}$ alloy is markedly lower than the others, 300 K at low coverage, decreasing to 275 K as the coverage is increased. For saturation coverage, two distinct desorption peaks are observed at 275 and 225 K. We found the D_2 desorption curves to be sensitive to the completion of the surface alloy layers, particularly for the $p(2\times2)$Sn/Pt(111) structure. Incomplete formation of the $p(2\times2)$ alloy surface results in areas of clean Pt(111) dominating sticking of D_2 and TPD spectra at low D atom coverage are characteristic of D_2 desorption from Pt, rather than from the $p(2\times2)$ alloy. For fractional Sn coverages between $\Theta_{Sn} = 0.25$ and 0.33, the surface is covered by areas of both $p(2\times2)$ and $\sqrt{3}$ alloy and the TPD spectra consist of desorption peaks from both surfaces.

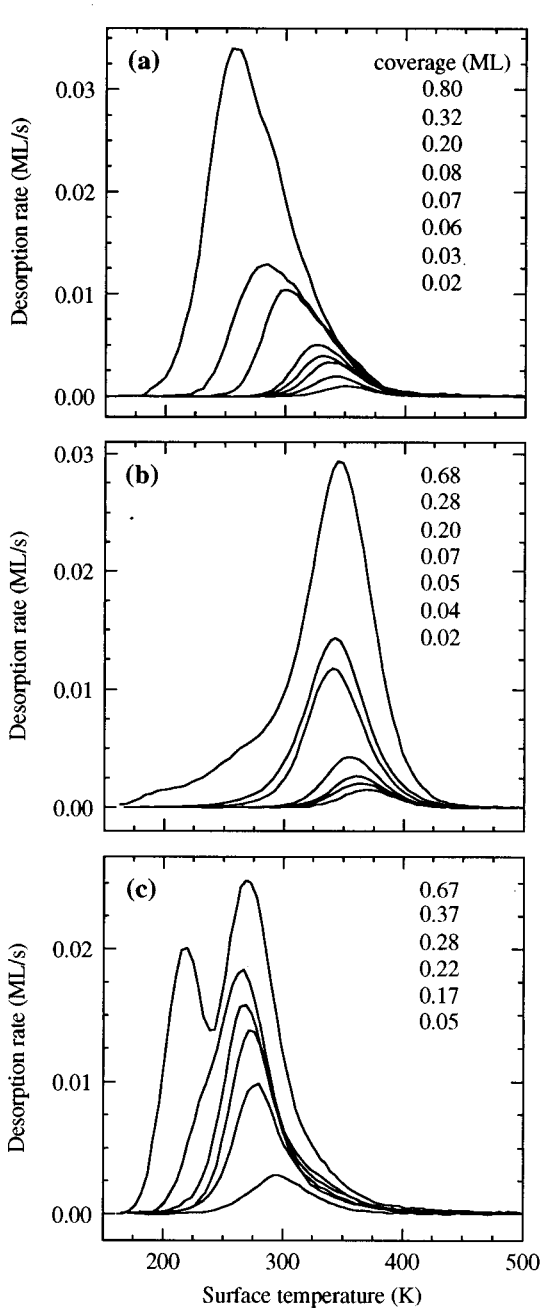

FIG. 2. Thermal desorption spectra of D_2 from (a) Pt(111), (b) $p(2\times2)$Sn/Pt(111), and (c) $(\sqrt{3}\times\sqrt{3})R30°$ Sn/Pt(111) as a function of initial D atom coverage, following exposure to a D_2 molecular beam at a surface temperature $T_s = 150$ K. The initial coverages have been determined from the relative areas of the desorption peaks, assuming a saturation D atom coverage of 0.8 ML on the Pt(111) surface. A constant heating rate of 3.5 K s^{-1} was used.

B. Kinetic analysis

In order to determine activation energies for D_2 desorption, TPD spectra have been measured as a function of heating rate and analyzed using the Taylor–Weinberg method.[23] The rate of desorption $R_d(\Theta_D, T_s)$ is assumed to follow a simple Polanyi–Wigner form,

$$R_d(\Theta_D, T_s) = -\frac{d\Theta_D}{dt} = \nu(\Theta_D)\Theta_D^n \exp\left[-\frac{E_d(\Theta_D)}{kT_s}\right], \quad (1)$$

TABLE I. Activation energies and desorption parameters for D_2 on Sn/Pt(111) alloy surfaces.

	Pt(111)	$p(2\times2)$Sn/Pt(111)	$(\sqrt{3}\times\sqrt{3})R30°$ Sn/Pt(111)
E_d (eV)	0.71±0.1	0.67±0.1	0.40±0.1
Preexponential ($cm^2\,atom^{-1}\,s^{-1}$)	4×10^{-5}	5×10^{-6}	1.3×10^{-8}

where Θ_D is the D atom coverage, n is the reaction order, $\nu(\Theta_D)$ is the preexponential factor and $E_d(\Theta_D)$ is the activation energy for desorption. The activation energy for desorption, E_d, comes directly from an Arrhenius plot of $\ln I(\Theta_D,T_s)$, where I is the QMS signal, against $1/T_s$ at a constant coverage Θ_D, without having to make any assumptions about the kinetic order of desorption or the dependence of E_d on coverage. Desorption parameters were measured for low coverage, those for Pt(111) in particular being sensitive to Θ_D, the activation barrier dropping rapidly with Θ_D and giving rise to an asymmetric peak shape. Values of E_d for D_2 desorption from Pt(111), $p(2\times2)$, and $\sqrt{3}$ alloys are shown in Table I and similar results were obtained by Voss *et al.*[21]

Order plots of $\ln I(\Theta_D,T_s)$ against $\ln\Theta_D$ at constant T_s showed that desorption was approximately second order, as expected from the common high-temperature edge of the desorption traces at low coverage. The TPD measurements from Pt(111) could be simulated assuming a coverage-dependent activation energy, $E_d(\Theta_D)=(0.7-0.3\Theta_D)$ eV, a coverage independent preexponential factor, $\nu=4\times10^{-5}$ $cm^2\,atom^{-1}\,s^{-1}$ and second-order desorption. For coverages below saturation, both the heating rate and coverage dependence of the TPD curves from the Sn/Pt(111) alloys can be modeled using the values of E_d determined from the low-coverage Taylor–Weinberg analysis, with second-order desorption kinetics and coverage independent preexponential factors of 5×10^{-6} $cm^2\,atom^{-1}\,s^{-1}$ for the $p(2\times2)$ alloy (Fig. 3) and 1.3×10^{-8} $cm^2\,atom^{-1}\,s^{-1}$ for the $\sqrt{3}$ surface alloy (Fig. 4). Agreement is reasonably good but at high coverages the desorption curves from the $p(2\times2)$ alloy show a slight asymmetry towards low temperatures, while the curves from the $\sqrt{3}$ alloy have a weak high-temperature tail (Fig. 2).

The activation barrier to desorption from the $p(2\times2)$ alloy is almost unchanged by the presence of 0.25 ML of Sn in the top layer compared to Pt(111). The alloy surface shows a slightly reduced preexponential factor for desorption, consistent with a more constrained site for desorption from the alloy surface. Formation of the $\sqrt{3}$ alloy with 0.33 ML Sn results in an abrupt decrease in the activation barrier to D_2 recombinative desorption and a further reduction in the preexponential factor compared to the Pt value. Since the preferred binding site for D is the threefold coordinated hollow site on Pt(111),[6,24] the abrupt change in desorption barrier on forming the $\sqrt{3}$, but not the $p(2\times2)$, surface alloy seems to be associated with loss of the stable threefold Pt site for the $\sqrt{3}$ alloy. This would be consistent with a reduced binding energy on the $\sqrt{3}$ surface as these sites are replaced by Pt_2Sn hollow sites. However, to establish the energetics of

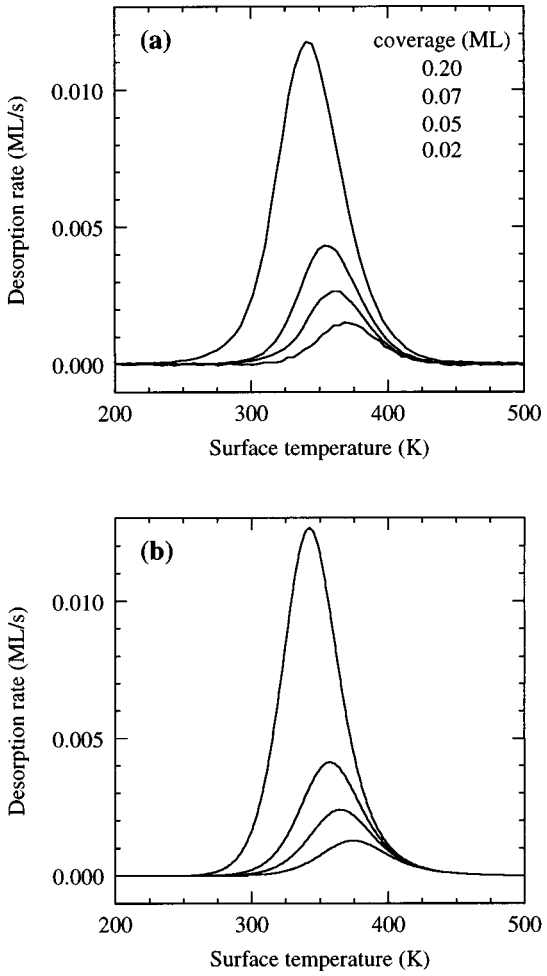

FIG. 3. (a) Experimental and (b) simulated D_2 TPD spectra from the $p(2\times2)$ alloy for different initial D atom coverages and a heating rate of 3.5 K s^{-1}. The simulated curves were calculated using second-order desorption kinetics, with a constant activation energy, $E_d=0.67$ eV, obtained from a Taylor–Weinberg analysis, and a preexponential factor, $\nu=5\times10^{-6}$ $cm^2\,atom^{-1}\,s^{-1}$.

adsorption the activation barrier to dissociative chemisorption must be determined and compared to the barrier for desorption. The principle of detailed balance implies that the reduction in the preexponential factors for desorption from the $p(2\times2)$ and $\sqrt{3}$ alloy surfaces must be matched by a reduction in the absolute probability for dissociative chemisorption on these surfaces, in addition to any changes in the activation barrier to dissociation.

C. Dissociative chemisorption

1. Sticking probability measurements on Pt(111) and $p(2\times2)$ Sn/Pt(111)

Initial sticking probabilities, S_0 in the limit of zero coverage, have been measured for a D_2 beam incident normal to the clean Pt(111) sample and the two Sn/Pt(111) surface alloys at a temperature $T_s=150$ K. Measurements were made for pure D_2 beams with nozzle temperatures in the range $T_n=295-1900$ K, corresponding to mean translational energies $70<E<450$ meV. Sticking probabilities on the $\sqrt{3}$ alloy

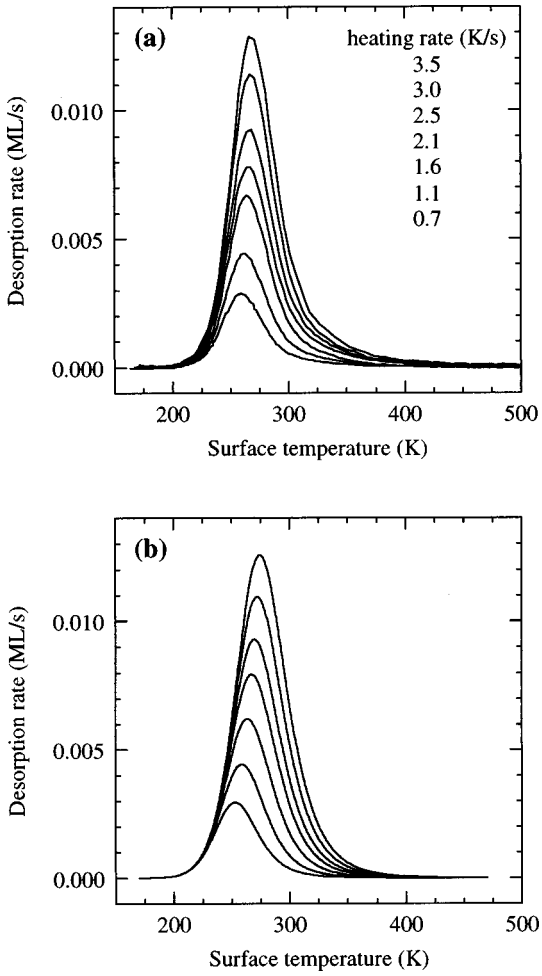

FIG. 4. (a) Experimental and (b) simulated D_2 TPD spectra from the $\sqrt{3}$ alloy for different heating rates and an initial D atom coverage of 0.21 ML. The simulated curves were calculated for second-order desorption kinetics, a constant activation energy, $E_d = 0.40$ eV, and a preexponential factor, $\nu = 1.3\times10^{-8}$ cm^2 atom^{-1} s^{-1}.

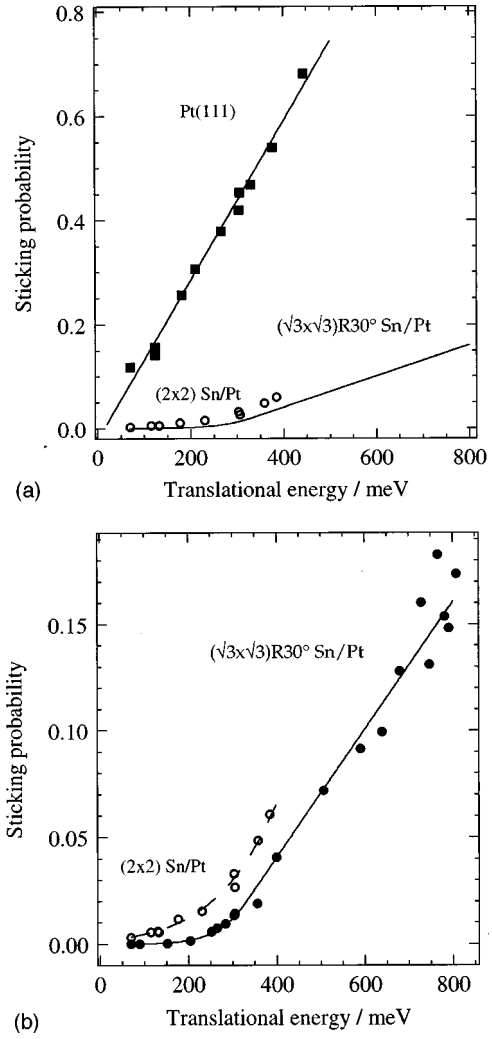

FIG. 5. (a) Initial sticking probability, S_0, for D_2 dissociative chemisorption on Pt(111) (■), $p(2\times2)$ (○), and $\sqrt{3}$ surface alloy (solid line), as a function of translational energy, E, on a 150 K surface. (b) Same as (a) but showing the $p(2\times2)$ (○ and dotted line) and $\sqrt{3}$ (● and solid line) data in more detail. The points above 450 meV were obtained by seeding D_2 in H_2 while the solid line through the $\sqrt{3}$ data is the result of a fit, described in Sec. III C 3, and the dotted line through the $p(2\times2)$ data is a simple superposition of a linear and activated behavior, described in Sec. III E.

were also made for incident energies $E>500$ meV, by seeding D_2 with H_2 at nozzle temperatures $1300<T_n<2050$ K, and as a function of incidence angle.

The dependence of sticking probability on the translational energy is shown for all three surfaces in Fig. 5. The $S_0(E)$ dependence on Pt(111) reproduces closely the previous results of Luntz *et al.*,[10] with the sticking probability increasing steadily from $S_0=0.12-0.68$, as the translational energy is increased from 70 to 440 meV. The $p(2\times2)$ alloy was difficult to prepare without small regions of either bare Pt(111) or $\sqrt{3}$ alloy, which made the sticking probability sensitive to surface preparation. If the alloy layer is incomplete sticking is dominated by clean Pt islands, so measurements on this surface were always carried out with a faint $(\sqrt{3}\times\sqrt{3})R30°$ contribution to the LEED pattern. Just as for Pt(111), dissociation on the $p(2\times2)$ alloy increases approximately linearly from zero energy up to ~250 meV but is a factor of ~30 lower than on bare Pt(111). Above ~250 meV the sticking probability on $p(2\times2)$ Sn/Pt(111) increases more rapidly. The possibility that sticking was still dominated by small regions of bare Pt(111) was explored by changing the surface composition to show increasing amounts of the $\sqrt{3}$ structure. We believe, from D_2 TPD measurements at low coverage, that the fraction of bare Pt is much less than the 4% required to interpret the residual sticking as bare Pt, however, our reported values may underestimate sticking for the $p(2\times2)$ surface by up to 20% due to the presence of islands of the $\sqrt{3}$ alloy. Dissociation on the $\sqrt{3}$ alloy is more strongly inhibited than for the $p(2\times2)$ structure, being more than three orders of magnitude lower than that on Pt(111) at $E=70$ meV. We describe the behavior of the $\sqrt{3}$ alloy below, before returning to discuss the behavior of the $p(2\times2)$ surface in the light of these results.

2. Dissociation on $(\sqrt{3}\times\sqrt{3})R30°$ Sn/Pt(111)

At translational energies above ~280 meV the sticking probability for the $\sqrt{3}$ alloy increases linearly with energy. This behavior looks similar to the linear $S_0(E)$ dependence on Pt(111), but shifted to a higher threshold and with a re-

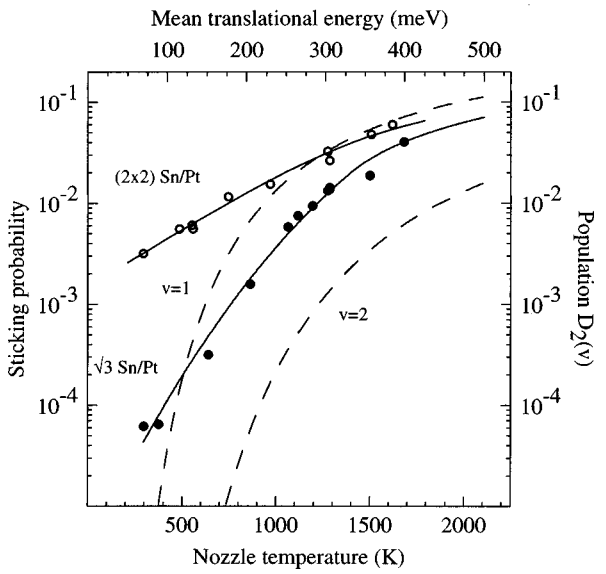

FIG. 6. Logarithmic plot showing the variation of the initial sticking probability, S_0, for D_2 dissociative chemisorption on $p(2\times2)$ (○) and $\sqrt{3}$ (●) alloys, at a surface temperature $T_s=150$ K, as a function of nozzle temperature, T_n, and incident translational energy, E. The relative populations $P(v)$ of the first two vibrationally excited states ($v=1,2$) of D_2 in the molecular beam are also plotted (dashed lines) as a function of nozzle temperature, T_n.

duced slope. Because sticking only becomes efficient at high energy, the dissociation probability for D_2 on the $\sqrt{3}$ alloy is comparable to the population of $D_2(v=1)$ in the molecular beam (Fig. 6). It is therefore possible that excited vibrational states $D_2(v\geqslant1)$ contribute substantially to sticking. However, dissociation cannot be due exclusively to excited vibrational states, since below 100 meV $S_0(E)$ is greater than the population of $D_2(v=1)$. Similarly, the measurements made with the seeded molecular beam $400\leqslant E\leqslant800$ (Fig. 7) correspond to nozzle temperatures $1300<T_n<2050$ K and S_0 is greater than the $D_2(v=1)$ population in this temperature range.

If sticking is dominated by vibrationally excited states, changing the normal translational energy ($E_\perp=E\cos^2\theta_i$) by varying the angle of incidence θ_i or by changing the nozzle temperature will have different effects on $S_0(E_\perp)$, since changing the nozzle temperature also changes the population of excited molecules. Thus if $S_0(E_\perp)$ is measured at a constant nozzle temperature by increasing θ_i, the values obtained will be larger than obtained at the same normal energy by dropping the nozzle temperature, since the latter decreases the population of vibrationally excited molecules in the beam. This is the behavior observed on Cu,[13,25] Ag,[14] and the (2×1) $Cu_{85}Pd_{15}(110)$[26] surfaces, where vibrationally excited states dominate sticking and $S_0(E_\perp)$ curves obtained for a constant nozzle temperature, by increasing θ_i, drop slowly by comparison with the normal incidence curve. Sticking probabilities on the $\sqrt{3}$ alloy were measured as a function of incidence angle at various fixed nozzle temperatures, in order to investigate the role of vibrational energy and the energy scaling relationship. Figure 7(a) shows three series of angular measurements, taken at incident energies $E=400$, 305, and 205 meV, in which S_0 is plotted against the normal component of the mean translational energy. At

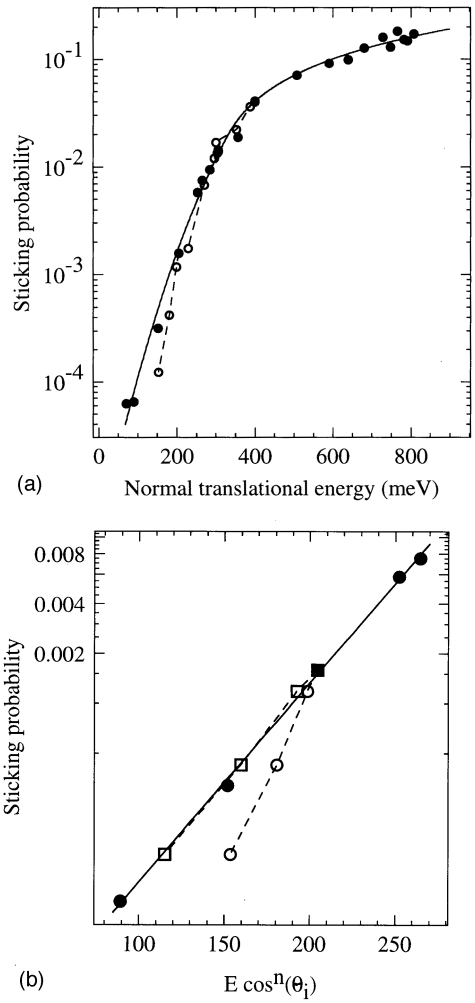

FIG. 7. (a) Dissociative chemisorption probability, S_0 of D_2 on $(\sqrt{3}\times\sqrt{3})R30°$ Sn/Pt(111), at a surface temperature $T_s=150$ K, as a function of the translational energy, E and incidence angle, θ_i. Sticking probabilities for $E>500$ meV were obtained using a D_2 molecular beam seeded with H_2, and nozzle temperatures in the range $1300<T_n<2050$ K. The solid line through the normal incidence data (●) is the result of a fit described in the text. Three series of angular measurements (○) for $E=400$, 305, and 205 meV are shown. (b) S_0 measured as a function of θ_i for $E=205$ meV is plotted against ($E\cos^n\theta_i$) for $n=2$ (○) and $n=4$ (□) in order to determine the energy scaling at low E.

high energy, the angular measurements follow the curve of the normal incidence ($\theta_i=0°$) data, indicating an approximately normal energy scaling. We could find no evidence, either from angular or from seeded beam measurements, that the internal state distribution of the beam played any significant role in determining $S_0(E)$ under our beam conditions. Ground state $D_2(v=0)$ dominates sticking across the entire energy range and contributions to S_0 from higher vibrational states can be ignored. We conclude that vibrational excitation of D_2 molecules does not promote sticking on $(\sqrt{3}\times\sqrt{3})R30°$ Sn/Pt(111) efficiently, if at all.

Rather than having an enhanced sticking probability, the angular measurements at low energy (Fig. 7) fall significantly below the $\theta_i=0°$ curve, implying that motion parallel to the surface suppresses dissociation. This is in complete contrast to what would be expected if excited states of D_2

were contributing to dissociation, in which case the $S_0(E,\theta_i>0)$ curve would lie above the $S_0(E,\theta_i=0)$ data. The inhibition is shown most clearly in the angular behavior at low energy, which is shown in detail for $E=205$ meV in Fig. 7(b). Fitting the angular data to an energy scaling parameter $n(E)$ such that $S_0(E,\theta_i)=S_0(E\cos^{n(E)}\theta_i,\theta_i=0°)$ gave $n=4$ at 205 meV, $n=2.6$ at 305 meV and a normal energy scaling ($n\sim2$) at higher energies.

The deviation from normal energy scaling observed in the $S_0(E,\theta_i)$ data at low E indicates that momentum parallel to the surface inhibits sticking when compared to molecules incident along the surface normal. Similar inhibition of dissociative chemisorption by parallel momentum has been observed before, most dramatically on Fe(110),[11,12] while on Pt(111) sticking seemed to be enhanced at small angles but was inhibited as θ_i increased.[10] Calculations for activated dissociation of H_2 on metal surfaces[27,28] have shown that the barrier to dissociation can be expected to depend sensitively on the site, varying both in magnitude and height above the surface at different sites in the unit cell. At low energy, momentum parallel to the surface can inhibit dissociation either by preventing the molecule from spending sufficient time at a favorable surface site or by preventing the molecule steering into the correct dissociation geometry at that site. Scattering calculations[29] have shown that if the magnitude of the barrier across the surface unit cell is corrugated then the dissociation process is inhibited by motion parallel to the surface. On the other hand corrugation of the vertical location of the barrier above the surface, referred to as geometric corrugation, has the opposite effect and together the two different types of corrugation can give rise to complex energy scaling behavior.[29,30] At high incident energies, the steric requirements for dissociative chemisorption relax, with a greater proportion of the molecules dissociating, and a normal energy scaling is observed. The energy scaling for sticking of D_2 on the $\sqrt{3}$ alloy is consistent with a strong site dependence to the dissociation barrier and inhibition of dissociation by motion parallel to the surface. This site dependence is exactly what one might expect if Sn locally inhibits dissociation and only particular Pt sites are active. The energy scaling on the $\sqrt{3}$ alloy is quite different to that for H_2 dissociation on Cu(111), which changes from a normal energy scaling at high energy ($n=2$) towards a total energy scaling ($n\rightarrow0$) at low energy,[31] consistent with a vertically corrugated potential.[29,30]

3. Models for $S(E)$ on $(\sqrt{3}\times\sqrt{3})R30°$ Sn/Pt(111)

Despite having a large activation barrier, the $S_0(E)$ dependence on the $\sqrt{3}$ alloy displays a different form to that for dissociation on the noble metals. On Cu[13,25] and Ag[14,32] dissociation is dominated by large activation barriers and the functional form of $S_0(E)$ can be modeled using ''S''-shaped sticking functions based on tanh or error function forms,

$$S_0(E)=\frac{A}{2}\left[1+\mathrm{erf}\left(\frac{E-E_0}{w}\right)\right], \tag{2}$$

where E_0 is the sticking ''threshold,'' w determines how sharply sticking increases, and A is the limiting high-energy sticking probability. However, this function does not give satisfactory fits to the data from the $\sqrt{3}$ alloy, which shows an exponential increase in $S(E)$ followed by a linear increase in $S(E)$ at higher energy, and cannot be described by any single values of E_0 and w. Despite the large barrier D_2 dissociation on the $\sqrt{3}$ alloy shows no evidence for vibrational enhancement, in contrast to other activated dissociative chemisorption systems such as H_2/D_2 on Cu,[13,25] $Cu_{85}Pd_{15}(110)(2\times1)$,[26] NiAl(110),[16] and Ag(111),[14] as well as dissociation of CH_4 (Ref. 33) and N_2 (Ref. 34) on metal surfaces.

Above a threshold of ~280 meV the functional form $S_0(E)$ resembles that observed for Pt(111) but with a reduced gradient. We interpret the linear increase in $S_0(E)$ at high energy as due to a distribution of different activation barriers within the unit cell for molecules with different initial orientations, the range of dissociation sites opening up as the incident energy is increased. Fitting the high-energy part of the curve to a straight line gives a sticking threshold of ~280 meV. On Ag(111) (Ref. 35) and Cu(111) (Refs. 31 and 36) the width, w, of the sticking functions is determined by the surface temperature, thermal motion of the surface broadening the distribution of barriers sampled by the incoming molecules. If we assume that the same mechanism applies on this surface then the exponential increase in $S(E)$ at low energy will be determined by thermal broadening of the barrier distribution. Sticking on the $\sqrt{3}$ alloy can be modeled by assuming a linear distribution of barriers $P(V)$, of height V, for energies greater than some threshold a_1, such that

$$P(V)=\begin{cases}0, & V<a_1\\ a_3, & V>a_1\end{cases}, \tag{3}$$

where the sticking function for each of these ''sites'' is broadened to low energy by the finite temperature of the sample.[35] If we take the broadening of the sticking function as defined by a single width parameter a_2, such that at a translational energy E the sticking probability for a given barrier height V is given by,

$$S(E,V)=\begin{cases}1, & E>V\\ [\exp\{(E-V)/a_2\}], & E<V,\end{cases} \tag{4}$$

for example, then we have a simple three parameter model for $S_0(E)$,

$$S_0(E)=\int_{a_1}^{\infty}P(V)S(E,V)dV, \tag{5}$$

where a_1 is the threshold, a_2 specifies the width of the thermal broadening, and a_3 is the rate at which the dissociation sites open up. Unlike simple error or tanh functions [Eq. (2)], this form gave an accurate fit to the sticking data across the entire energy range. Values of the parameters were obtained from a fit to the experimental $S_0(E)$ data, shown as the solid line through the data in Figs. 5–7, with parameters $a_1=289$ meV, $a_2=40.6$ meV, and $a_3=2.8\times10^{-4}$ meV^{-1}.

D. Energetics of D_2 adsorption

It is possible to provide estimates of the binding energy for D on the Sn/Pt alloy surfaces by comparing the activation

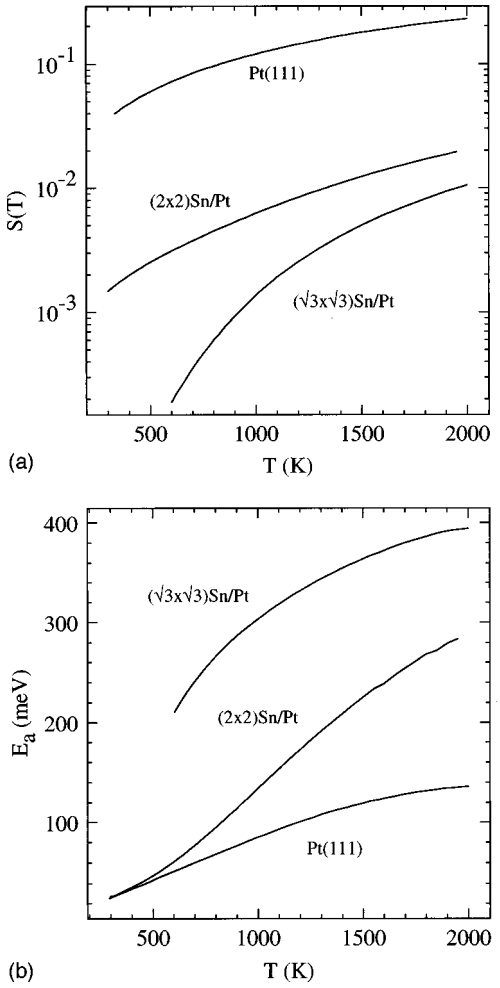

FIG. 8. (a) Calculated sticking probability for a Maxwellian gas with a translational temperature, T, on 150 K Sn/Pt(111) surfaces. (b) Arrhenius activation energies for dissociative chemisorption of D_2 as a function of the translational temperature of the gas.

barriers for recombinative desorption (E_d) and dissociative chemisorption (E_a) of D_2. To do this this we need to calculate the Arrhenius activation energy for D_2 dissociative chemisorption from the sticking data, at the temperature where desorption occurs. The thermal sticking probability, $S(T_g)$ for a gas at a temperature T_g on the 150 K surface, can be calculated by integrating the sticking probabilities over an isotropic Maxwellian energy distribution.[37] This procedure assumes that sticking is dominated by translational activation of the gas and that $S(E)$ is roughly independent of the surface temperature. For Pt(111) and the $p(2\times2)$ alloy a linear fit to $S(E)$ and a normal energy scaling were used for $S(E,\theta_i)$. The sticking functions $S(T_g)$ and the resulting Arrhenius activation energies for D_2 dissociation are shown in Fig. 8. At 300 K the Arrhenius activation energies for Pt(111) and $p(2\times2)$ Sn/Pt(111) are low, reflecting the linear increase in $S(E)$ at low energies. The activation energy for the $p(2\times2)$ alloy rises at higher gas temperatures as sticking starts to occur via a more activated channel [Fig. 5(b)] at $E>250$ meV. Combining the activation energies for D_2 dissociation and desorption (Table I) gives estimates of (0.68 ± 0.1) and (0.64 ± 0.1) eV for the energy release during dissociative chemisorption on the Pt(111) and $p(2\times2)$ alloy surfaces, in good agreement with a value of 0.69 eV for the low coverage isosteric heat of adsorption on Pt(111).[22] This gives a D binding energy of (251 ± 5) and (249 ± 5) kJ mol^{-1} on Pt(111) and $p(2\times2)$ alloy surfaces, respectively.

For the $\sqrt{3}$ alloy the sticking function described above was used to give the $S(E)$ dependence while the angular dependence was mimicked by assuming that the energy scaling parameter increased at low energy, in line with the results presented in Sec. III C. Different assumptions about the variation $n(E)$ at low energy give increasing uncertainty to the calculated $S(T_g)$ at $T_g<750$ K, at which energies the sticking data is becoming sparse. The data has been truncated below 750 K where the calculated $S(T_g)$ begins to rely on extrapolation of the $S(E)$ data. The calculated activation energy for D_2 dissociation on the $\sqrt{3}$ alloy is much larger than for Pt(111) or the $p(2\times2)$ alloy, and varies somewhat with temperature, being similar to the threshold of ~0.28 eV where sticking becomes facile. For H_2 dissociation on Cu(111) we have recently shown that thermal motion of the metal surface becomes increasingly important in activating dissociation as the translational energy drops below the threshold for efficient sticking.[31] The effect of surface thermal motion is ignored in this calculation, since we cannot measure sticking data over a wide range of T_s, and so we expect the calculated values of E_a to become increasingly unreliable as the gas temperature decreases and sticking becomes small. In view of this we use the sticking threshold (a_1) to give an estimate of $E_a=(0.28\pm0.1)$ eV,[38] yielding a heat of adsorption of (0.12 ± 0.2) eV and a binding energy of (224 ± 10) kJ mol^{-1} for D on the $\sqrt{3}$ alloy.

The change in the D binding energy correlates well with the presence of stable threefold hollow Pt sites on the surface, the binding energy being almost identical for Pt(111) and $p(2\times2)$Sn/Pt(111) at low coverages. The implication is that the presence of Sn atoms adjacent to the Pt_3 units on the $p(2\times2)$ surface has minimal effect on the electronic structure of the D binding site. In contrast on the $\sqrt{3}$ alloy these Pt_3 sites are lost, all the hollow sites being Pt_2Sn units (Fig. 1), and the heat of adsorption drops by about 0.5 eV with dissociation becoming almost thermoneutral. Since little structural data is available for D on the Sn/Pt(111) surface alloys, it is not certain whether the binding site remains the hollow site or whether Sn forces the D atoms into Pt bridge or atop sites. A high-resolution core level photoelectron study of this surface[39] showed that while the Sn sites were unaffected by H adsorption, the Pt showed a new surface component and it was suggested that H is adsorbed on the Pt, possibly in an atop site.

E. Discussion

Two mechanisms can be proposed by which the surface chemistry can be altered by alloying with another metal. The first is a geometric mechanism, in which the second component simply acts by blocking sites, thereby reducing the number of reactive sites at the surface and reducing the prefactors for reaction. The second is an electronic mechanism, whereby substitution of the second metal modifies the electronic structure of the dissociation sites and the stability of

the adsorbate.[6,7] Changes to the electronic structure of the surface will generally modify both the activation barriers and the steric constraints on the dissociation geometries. In general these two mechanisms will occur together and a clear distinction between the two is impossible, however, it is often conceptually useful to assume this separation is valid and that one effect or the other dominates.

Although dissociation is activated on both Pt(111) and $p(2\times2)$ alloy surfaces, the sticking probability increases steadily with translational energy, indicating that some sites and geometries have no barrier to dissociation. The abrupt change in the D binding energy as the surface composition reaches Pt_2Sn is mirrored by an increase in the dissociation threshold to ~280 meV on the $\sqrt{3}$ alloy. Once above threshold the dissociation probability increases steadily with energy for all three surfaces, as different sites and molecular geometries become important. This is not well represented by a simple ''S''-shaped sticking function but requires an energy threshold and separate widths to be specified for the region above threshold, where sticking is efficient, as well as below it where $S(E)$ dies exponentially. The behavior of the $p(2\times2)$ Sn/Pt(111) surface alloy appears to be a composite of the Pt(111) and $\sqrt{3}$ alloy behavior, with weakly activated dissociation occurring at low energies followed by an abrupt increase in sticking at around the same energy threshold as for the $\sqrt{3}$ alloy. The dotted curve through the $p(2\times2)$ sticking data of Fig. 5(b) shows the result of superimposing a linear increase in $S(E)$, but with a probability reduced by a factor of ~30 compared to the Pt(111) surface, with the activated behavior of the $\sqrt{3}$ alloy. The inhibition of H_2/D_2 dissociation on the Sn/Pt(111) alloy surfaces[17,20] is therefore attributed to an enhanced steric requirement for dissociation on the $p(2\times2)$ alloy at low energy and a second dissociation channel, which opens on both alloy surfaces at higher energies, with an energy threshold of ~280 meV and a severe steric constraint.

Calculations of the barrier for activated dissociation on Cu have shown a strong correlation between the site for activated dissociation and the most stable binding site for the atomic products.[27,28,40,41] Dissociation on Cu(111) has a minimum activation barrier for H_2 lying parallel to the surface in the bridge geometry and dissociating into the hollow sites.[27] By contrast, on Cu(100) the minimum barrier geometry has one atom displaced towards the fourfold hollow site with the other tilted up towards the bridge site, which also has a reasonably favorable binding energy,[41] but requires a larger bond extension to reach the transition state.[42,43] Other low-energy dissociation paths on the Cu(111) surface include the atop to hollow site, whereas dissociation of D atoms into the unfavorable atop sties has a much larger barrier. Dissociation with the D_2 axis parallel to the surface, at an atop site, shows no activation barrier on Pt(111), consistent with the absence of an energy threshold in experiments.[6] The effect of alloying on the energetics of dissociation has been investigated in several LDA studies. Hammer and Nørskov investigated the barrier for dissociation on an ordered Cu_3Pt alloy, consisting of isolated, reactive Pt atoms surrounded by Cu.[6] The barrier to dissociation on the Cu sites increased while that on the Pt sites remained nonactivated, although the final adsorption sites were destabilized.

The reduction in stability of D atoms on the $\sqrt{3}$ alloy, and the abrupt increase in activation barrier to dissociation, occurs as the Pt_3 hollow sites are lost. This change in binding energy is consistent with a change in adsorption site from the stable Pt_3 hollow site on Pt(111) and $p(2\times2)$ surfaces, to a Pt bridge or atop site on the $\sqrt{3}$ alloy.[39] The presence of a weakly activated path on the $p(2\times2)$ alloy indicates that favored dissociation geometries remain, although with a greatly reduced probability due to the constraints imposed on the dissociation site. Although the bridge to threefold hollow Pt_3 site is lost on the $p(2\times2)$ surface, one of the D atoms dissociating into a Pt_2Sn site, the atop Pt to threefold hollow Pt_3 site is still available. This geometry appears to have no barrier in calculations on Pt(111) (Ref. 6) while on Cu this geometry has a similar barrier to the bridge to hollow dissociation path.[27] In agreement with this picture we find the steric requirements for dissociation on $p(2\times2)$ Sn/Pt(111) are increased, as evidenced by a reduced preexponential factor for recombinative desorption and a reduction in the sticking probability for dissociation at low-energy compared to Pt(111). Nevertheless, some nonactivated dissociation geometries remain, despite any modification of the electronic structure by neighboring Sn atoms. For dissociation on the $\sqrt{3}$ alloy the presence of three neighboring Sn atoms for each Pt atom has shifted the threshold up to ~0.28 eV. The threefold Pt_3 sites are lost and dissociation presumably occurs either into the less stable atop Pt sites[39] or, via a lower symmetry path, into Pt_2 bridge sites. Deuterium adsorption is ~0.5 eV less favorable than on Pt(111) or the $p(2\times2)$ alloy surface, dissociation being only slightly exothermic, just as on Cu. The blocking behavior of the Sn atoms results in a strong steric requirement on the dissociation site for the $\sqrt{3}$ alloy, dissociation being confined to geometries which result in favorable D binding sites. Unlike Cu, the absence of vibrational enhancement indicates that the barrier remains in the entrance channel before the D_2 bond stretches significantly. Dissociation at higher energies on the $p(2\times2)$ alloy shows a similar threshold behavior around 280 meV, suggesting that dissociation sites associated with the Pt_2Sn units of the $\sqrt{3}$ alloy surface are also becoming available on the $p(2\times2)$ surface at a similar energy.

F. Conclusions

The adsorption–desorption dynamics of D_2 on Sn/Pt(111) surface alloys show a strong dependence on the local surface structure which we have investigated by comparing the energetic and steric requirements for both processes. Initially, for $\Theta_{Sn}=0.25$ ML on the $p(2\times2)$ alloy, the transition state becomes more constrained and this is reflected in the decreased prefactor for recombinative desorption and the reduced slope of $S(E)$. As the Sn coverage is increased to 1/3 ML on the $\sqrt{3}$ alloy, the Pt_3 hollow sites are lost and the D binding energy falls to $224\ \mathrm{kJ\,mol^{-1}}$, compared to $250\ \mathrm{kJ\,mol^{-1}}$ on the Pt(111) and $p(2\times2)$ alloy surfaces. Dissociation on the $\sqrt{3}$ alloy is activated with a sticking threshold of ~280 meV. At the same time the steric requirements on the dissociation site become even more severe, as

evidenced by a further reduction in the preexponential factor for desorption and low sticking probabilities even at energies well above threshold. This is consistent with a tightly constrained transition state, only molecules which collide at the right site and with the correct orientation being able to dissociate. By analogy with the trends observed in LDA calculations we suggest that the favored dissociation sites are those that lead directly to D bound in the stable Pt_3 hollow sites. Despite a barely exothermic dissociation process, (0.12 ± 0.2) eV, and a substantial activation barrier, no vibrational effects were seen and the barrier to dissociation on the $\sqrt{3}$ alloy remains in the entrance channel before the D_2 bond begins to stretch.

[1] P. M. Holmblad, J. H. Larsen, and I. Chorkendorff, J. Chem. Phys. **104**, 7289 (1996).
[2] M. T. Paffett and R. G. Windham, Surf. Sci. **208**, 34 (1989).
[3] S. H. Overbury, D. R. Mullins, M. T. Paffett, and B. E. Koel, Surf. Sci. **254**, 45 (1991).
[4] A. Atrei, U. Bardi, J. X. Wu, E. Zanazzi, and G. Rovida, Surf. Sci. **290**, 286 (1993).
[5] M. Galeotti, A. Atrei, U. Bardi, G. Rovida, and M. Torrini, Surf. Sci. **313**, 349 (1994).
[6] B. Hammer and J. K. Nørskov, Surf. Sci. **343**, 211 (1995).
[7] B. Hammer and M. Scheffler, Phys. Rev. Lett. **74**, 3487 (1995).
[8] K. Christmann, Surf. Sci. Rep. **9**, 1 (1988).
[9] K. D. Rendulic, G. Anger, and A. Winkler, Surf. Sci. **208**, 404 (1989).
[10] A. C. Luntz, J. K. Brown, and M. D. Williams, J. Chem. Phys. **93**, 5240 (1990).
[11] A. Hodgson, A. Wight, G. Worthy, D. Butler, and B. E. Hayden, Faraday Discuss. **96**, 161 (1993).
[12] A. Wight, A. Hodgson, G. Worthy, D. Butler, and B. E. Hayden, Surf. Rev. Lett. **1**, 693 (1994).
[13] C. T. Rettner, D. J. Auerbach, and H. A. Michelsen, Phys. Rev. Lett. **68**, 1164 (1992).
[14] C. Cottrell, R. N. Carter, A. Nesbitt, P. Samson, and A. Hodgson, J. Chem. Phys. **106**, 4714 (1997).
[15] H. F. Berger and K. D. Rendulic, Surf. Sci. **253**, 325 (1991).
[16] M. Beutl, K. D. Rendulic, and G. R. Castro, J. Chem. Soc., Faraday Trans. **91**, 3639 (1995).
[17] H. Verbeek and W. H. Sachtler, J. Catal. **42**, 257 (1976).
[18] C. Xu and B. E. Koel, Surf. Sci. **304**, 249 (1994).
[19] K. Christmann, G. Ertl, and T. Pignet, Surf. Sci. **54**, 365 (1976).
[20] M. T. Paffett, S. C. Gebhard, R. G. Windham, and B. E. Koel, J. Phys. Chem. **94**, 6831 (1990).
[21] M. R. Voss, H. Busse, and B. E. Koel (submitted).
[22] P. R. Norton, J. A. Davies, and T. E. Jackson, Surf. Sci. **121**, 103 (1982).
[23] J. L. Taylor and W. H. Weinberg, Surf. Sci. **78**, 259 (1978).
[24] K. Mortensen, F. Besenbacher, I. Stensgaard, and C. Klink, Surf. Sci. **211/212**, 813 (1989).
[25] C. T. Rettner, H. A. Michelsen, and D. J. Auerbach, J. Chem. Phys. **102**, 4625 (1995).
[26] C. Cottrell, M. Bowker, A. Hodgson, and G. Worthy, Surf. Sci. **325**, 57 (1995).
[27] B. Hammer, M. Scheffler, K. W. Jacobsen, and J. K. Nørskov, Phys. Rev. Lett. **73**, 1400 (1994).
[28] J. A. White and D. M. Bird, Chem. Phys. Lett. **213**, 422 (1993).
[29] G. R. Darling and S. Holloway, Surf. Sci. **304**, L461 (1994).
[30] A. Gross, J. Chem. Phys. **102**, 5045 (1995).
[31] M. J. Murphy and A. Hodgson, J. Chem. Phys. **108**, 4199 (1998).
[32] F. Healey, R. N. Carter, G. Worthy, and A. Hodgson, Chem. Phys. Lett. **243**, 133 (1995).
[33] S. G. Brass and G. Ehrlich, Surf. Sci. **191**, L819 (1987).
[34] C. T. Rettner and H. Stein, Phys. Rev. Lett. **59**, 2768 (1987).
[35] M. J. Murphy and A. Hodgson, Phys. Rev. Lett. **78**, 4458 (1997).
[36] C. T. Rettner, H. A. Michelsen, D. J. Auerbach, and C. B. Mullins, J. Chem. Phys. **94**, 7499 (1991).
[37] C. T. Rettner, H. A. Michelsen, and D. J. Auerbach, Faraday Discuss. Chem. Soc. **96**, 17 (1993).
[38] R. D. Levine and R. D. Bernstein, *Molecular Reaction Dynamics and Chemical Reactivity* (Oxford University Press, Oxford, 1987).
[39] E. Janin, M. Björkqvist, T. M. Grehk, M. Göthelid, C. Pradier, U. O. Karlsson, and A. Rosemgren, Appl. Surf. Sci. **99**, 371 (1996).
[40] P. J. Feibelman, Phys. Rev. Lett. **67**, 461 (1991).
[41] J. A. White, D. M. Bird, M. C. Payne, and I. Stich, Phys. Rev. Lett. **73**, 1404 (1994).
[42] P. Kratzer, B. Hammer, and J. K. Nørskov, Surf. Sci. **359**, 45 (1996).
[43] G. Wiesenekker, G. J. Kroes, and E. J. Baerends, J. Chem. Phys. **104**, 7344 (1996).